

- Merril, C. R., Goldman, D., Sedman, S. A., & Ebert, M. H. (1981) *Science* 211, 1437-1438.
- Nagata, K., Matsunaga, T., Gillette, J., Gelboin, H. V., & Gonzalez, F. J. (1987) *J. Biol. Chem.* 262, 2787-2793.
- Nebert, D. W., & Gonzalez, F. J. (1987) *Annu. Rev. Biochem.* 56, 945-993.
- Nebert, D. W., Nelson, D. R., Adesnik, M., Coon, M. J., Estabrook, R. W., Gonzalez, F. J., Guengerich, F. P., Gunsalus, I. C., Johnson, E. F., Kemper, B., Levin, W., Phillips, I. R., Sato, R., & Waterman, M. R. (1989) *DNA* 8, 1-13.
- Nef, P., Heldman, J., Lazard, D., Margalit, T., Jaye, M., Hanukoglu, I., & Lancet, D. (1989) *J. Biol. Chem.* 264, 6780-6785.
- Phillips, I. R. (1986) *Biochem. Soc. Trans.* 15, 573-589.
- Phillips, I. R., Shephard, E. A., & Ashworth, A. (1985) *Proc. Natl. Acad. Sci. U.S.A.* 82, 983-987.
- Reed, C. J., Lock, E. A., & Di Matteis, F. (1986) *Biochem. J.* 240, 585-592.
- Siest, G., Antoine, B., Fournel, S., Magdalou, J., & Thomassin, J. (1987) *Biochem. Pharmacol.* 36, 983-989.
- Tephly, T. R., Green, M. D., Puig, J. F., & Irshaid, Y. M. (1988) *Xenobiotica* 18, 1201-1210.

Fluorescence and NMR Investigations on the Ligand Binding Properties of Adenylate Kinases

Jochen Reinstein,* Ingrid R. Vetter, Ilme Schlichting, Paul Rösch, Alfred Wittinghofer, and Roger S. Goody
Abteilung Biophysik, Max-Planck-Institut für medizinische Forschung, Jahnstrasse 29, 6900 Heidelberg, West Germany

Received August 16, 1989; Revised Manuscript Received April 2, 1990

ABSTRACT: A new system for measurement of affinities of adenylate kinases (AK) for substrates and inhibitors is presented. This system is based on the use of the fluorescent ligand α,ω -di[(3' or 2')-O-(N-methylanthraniloyl)adenosine-5'] pentaphosphate (mAP5Am), which is an analogue of the bisubstrate inhibitor diadenosine pentaphosphate (AP5A). It allows the determination of dissociation constants for any ligand in the range of 1×10^{-9} to 5×10^{-2} M. Affinities for different bisubstrate inhibitors (AP4A, AP5A, AP6A) and substrates (AMP, ADP, ATP, GTP) were determined in the presence and absence of magnesium. An analysis of the binding of bisubstrate inhibitors is proposed and applied to these data. The techniques are used to describe the properties of a mutant enzyme with Gln-28 \rightarrow His (Q28H) prepared by site-directed mutagenesis in comparison to those of wild-type AK from *Escherichia coli*. This newly introduced histidine is already present in most other adenylate kinases and was regarded to be important or even essential for the catalytic reaction of AK. Temperature denaturation experiments indicate that the mutant enzyme has the same thermal stability as the wild-type enzyme and, as NMR studies indicate, also a very similar structure. However, steady-state catalytic studies and binding experiments showed that the affinities for substrates and inhibitors are elevated from 3-fold (AMP) to 5-fold (ATP) to 15-fold (AP5A) compared to those of the wild-type enzyme. Together with the results obtained by Tian et al. [Tian, G., Sanders, C. R., Kishi, F., Nakazawa, A., & Tsai, M.-D. (1988) *Biochemistry* 27, 5544-5552] on the effect of replacement of the conserved His-36 in the cytosolic AK (AK1) from chicken by glutamine and asparagine, this shows that residues 28 of AK from *E. coli* (AKec) and 36 of AK1 are situated in a comparable environment and are not essential for catalytic activity.

The enzyme adenylate kinase (AK)¹ catalyzes the transfer of the γ -phosphate group of the "phosphate donor" (Mg-ATP) to the "phosphate acceptor" (AMP). It is one of the smallest phosphotransferases yet known. The ubiquitous presence of highly homologous forms of this enzyme in many different organisms reflects its important role in maintaining the energy charge of cells (Noda, 1973; Schulz et al., 1986). It was shown

by Konrad (1988) that disruption of the yeast *adk1* gene did not affect viability of the cells but that it is needed for normal cell proliferation. The fact that these cells still have about 10% of adenylate kinase activity compared to wild-type cells leads to the question of whether AK is absolutely essential for cell metabolism.

The mammalian cytosolic forms of pig and rabbit adenylate kinases (AK1) obey a random bi-bi rapid equilibrium kinetic mechanism, where the rate-limiting steps in catalysis were assigned to interconversion of the ternary complex between protein and substrates (Su & Russell, 1968) or to the dissociation of products (Rhoads & Lowenstein, 1968) from the protein. The stereochemical course of the catalyzed reaction was shown to follow an S_N2 mechanism, which suggests a direct transfer of the phosphoryl group without covalent enzymatic intermediates (Richard & Frey, 1978).

Despite the fact that numerous NMR experiments have been performed [Rösch et al., 1989; McDonald & Cohn, 1975; Nageswara Rao & Cohn, 1978; for a review, see Mildvan

¹ Abbreviations: AK, adenylate kinase (EC 2.7.4.3); AKec, adenylate kinase from *E. coli*; AKy, adenylate kinase from yeast; AK1, mammalian cytosolic enzyme; AMP, ADP, and ATP, adenosine 5'-mono-, 5'-di-, and 5'-triphosphate; APnA, Pⁱ, P^m-di(adenosine-5') n-phosphate; mAP5Am, α,ω -di[(3' or 2')-O-(N-methylanthraniloyl)adenosine-5'] pentaphosphate; mAP5A, α -[(3' or 2')-O-(N-methylanthraniloyl)adenosine-5'] ω -(adenosine-5') pentaphosphate; mdATP, 3'-O-(N-methylanthraniloyl)-2'-deoxyadenosine 5'-triphosphate; BSA, bovine serum albumin; EDTA, ethylenediaminetetraacetate; CD, circular dichroism; NMR, nuclear magnetic resonance; SDS, sodium dodecyl sulfate; Tris, tris(hydroxymethyl)aminomethane; DSS, sodium 4,4-dimethyl-4-silapentane-1-sulfonate; Q28H, mutant adenylate kinase from *E. coli* with a Gln-28 \rightarrow His substitution.

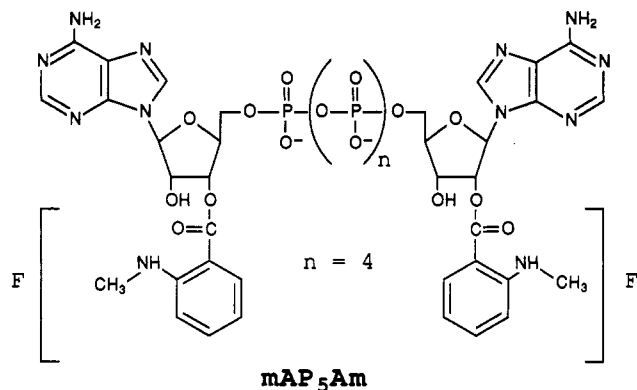


FIGURE 1: Structural formula of mAP₅Am; F = chromophore.

(1989)] and the crystal structures of three adenylate kinases (AK1 pig, AKy, and AKec) have been solved (Schulz et al., 1974; Egner et al., 1987; Müller & Schulz, 1988; Schulz et al., unpublished results), the spatial assignment of the substrate binding sites is still a subject of controversy. Direct assignment of the binding sites on the enzyme by X-ray crystallography has not been possible because of the difficulty of obtaining cocrystals with substrates. The determination of the three-dimensional structures of AKy and AKec in the presence of the inhibitor AP5A did not settle the issue because AP5A is a symmetrical molecule and it is not even certain that it is a genuine bisubstrate inhibitor which has its adenine rings located in the proper binding sites of AMP and Mg-ATP.

An interpretation of the structural findings with this symmetric "bisubstrate" analogue will be improved by the combination of two methods: (1) tagging of functionally important amino acids by site-directed mutagenesis and (2) detailed analysis of the binding parameters of substrates as well as bisubstrate inhibitors of the general formula AP_nA ($n = 4, 5, 6$) to wild-type and mutant proteins. Comparison of these binding data will improve the knowledge of the binding mode of AP5A.

Here we report the use of a versatile system for the measurement of binding constants for AK-ligand complexes. This system, which is based on the use of fluorescent derivatives of AP5A (mAP5A and mAP5Am), one of which is shown in Figure 1, allows the measurement of binding constants in the range of 2×10^2 to 1×10^9 M⁻¹. We use this system to evaluate the kinetic and binding characteristics of wild-type and a mutant (Q28H) adenylate kinase from *Escherichia coli* in detail.

Alignment of the conserved amino acid sequences of the adenylate kinase family (Haase et al., 1989; Schulz et al., 1986) shows that His-36 (numbering of AK1) is highly conserved in nearly all adenylate kinases. It was therefore surprising to find that adenylate kinase from *E. coli* has a glutamine residue at this position (number 28 according to the numbering of AKec) (Brune et al., 1986) since this histidine was implicated to be important or even essential for catalysis, mainly on the basis of X-ray structural analysis (Schulz et al., 1974; Pai et al., 1977) or NMR experiments with substrates (McDonald et al., 1975). Recently, a second adenylate kinase (*Paracoccus denitrificans*) was reported to have a glutamine residue (Gln-30) at the appropriate position by Spürgin et al. (1989). Tian et al. (1988) have shown that the mutation of His-36 to Gln or Asn results only in moderately elevated (about 7–10-fold) K_m values but nearly unaltered catalytic rate constants. Although this residue (His-36) is obviously not essential for the catalytic reaction of AKec, it was nevertheless interesting to see the effects of "reverting" Gln-28 of AKec to His.

MATERIALS AND METHODS

Strains and Plasmids. JM101 (Yanisch-Perron et al., 1985) was obtained by T. F. Meyer. SMH50 (Taylor et al., 1985) was obtained from F. Eckstein. M13mp9rev, BMH71-mutS, and MK30-3 (Kramer et al., 1984) were kindly provided by W. Kramer. The plasmid pEAK90 contains the *adk* gene and is a derivative of pEMBL9 (Dente et al., 1983) as described earlier (Reinstein et al., 1988).

Cloning Methods. Restriction enzymes, deoxynucleotides, and T4 DNA ligase were obtained from Boehringer Mannheim. DNA polymerase I large fragment (Klenow fragment) was from New England Nuclear. Enzyme buffers were used according to Maniatis et al. (1982). For transformation with DNA, cells were treated with CaCl₂ according to Mandel and Higa (1970).

Synthesis and Purification of Oligonucleotides. Oligonucleotides were synthesized according to the phosphoramidite method with a DNA synthesizer (Cyclone Bioscience). Products were purified in a two-step HPLC procedure using a C18-ODS column and the following parameters: flow rate, 2 mL/min; elution gradient, 20–40% acetonitrile in 100 mM triethylammonium acetate (TEA) over 20 min for the dimethoxytrityl-protected oligonucleotide and 5–20% acetonitrile over 30 min for the detritylated oligonucleotide.

Site-Directed Mutagenesis. Mutagenesis was carried out with M13mp9 containing the *adk* gene according to the gapped-duplex method (Kramer et al., 1984) essentially as described. The oligonucleotide used has the sequence 3'-TAA GGC GTG TAG AGG TG-5' and hybridizes to the coding (+)-strand of adenylate kinase, thus promoting a CAA to CAC transversion (His to Gln). From phage plaques obtained after the mutagenesis reaction, ssDNA was prepared and sequenced with the chain termination method (Sanger et al., 1977). Two out of eight plaques were positive, and from one of these dsDNA was prepared and exchanged for the corresponding *Hind*III-*Bst*EII wild-type fragment in pEAK90. The sequence of the resulting mutated pEAK plasmid was verified in the region of the mutated fragment by the chemical modification method (Maxam & Gilbert, 1980) using a solid support as described (Rosenthal et al., 1986).

Protein Purification. Proteins were prepared essentially as described (Reinstein et al., 1988) on a Blue Sepharose affinity column (Thompson et al., 1975) and a DEAE ion-exchange column.

Synthesis and Analysis of Fluorescent Nucleotide Analogues. AP5A was prepared by condensation of ADP with ATP that had been activated by reaction with carbonyldiimidazole as described by Hoard and Ott (1965) for the activation of monophosphates.

mAP5A and mAP5Am could be prepared in one reaction mixture. AP5A (0.8 mmol) was dissolved in water (10 mL), and the pH was brought to ca. 9.6 with dilute NaOH. Methylisatoic acid anhydride (2.4 mmol) was added and the temperature raised to ca. 40 °C. The pH changed toward neutral over the next 10–20 min; the mixture was titrated to ca. 9.6 by addition of dilute NaOH every few minutes. After the pH was constant, a further 0.8 mmol of methylisatoic acid anhydride was added, followed by further addition of dilute NaOH. This was repeated until a total of 5.6 mmol had been added over a period of ca. 3 h. The mixture was then applied to a column of Q-Sepharose Fast Flow equilibrated with 50 mM triethylammonium bicarbonate (pH 7.5), which was developed with a gradient of the same buffer (0.3–0.5 M), followed by isocratic elution with 0.5 M). The first major nucleotide peak eluted was unreacted AP5A (10.3%), the

second mAP5A (29.0%), and the third mAP5Am (28.3%). The proportions of mAP5A and mAP5Am could be changed by varying the excess of methylisatoic anhydride. The derivatives were characterized by their UV spectra, which showed peaks at 258 and 359 nm. The extinction coefficients were determined after cleavage with snake venom phosphodiesterase to the monophosphates (shown by TLC to be a mixture of mAMP and AMP in the case of mAP5A and to be mAMP only in the case of mAP5Am), whose extinction coefficients are known. The derivatives exhibited hypochromicities of 10% (mAP5A) and 11% (mAP5Am) at 258 nm, leading to calculated values for the extinction coefficients of $35\,600\text{ cm}^{-1}\text{ M}^{-1}$ (258 nm) and $4700\text{ cm}^{-1}\text{ M}^{-1}$ (359 nm) for mAP5A and $42\,000\text{ cm}^{-1}\text{ M}^{-1}$ (258 nm) and $9600\text{ cm}^{-1}\text{ M}^{-1}$ (359 nm) for mAP5A.

Analysis of Nucleotides. Purity of nonfluorescent nucleotides was assayed as described in Reinstein et al. (1988) with reversed-phase HPLC.

Binding Studies with Fluorescent Analogues. Fluorescence measurements were performed with an SLM Smart 8000 photon-counting spectrofluorometer. The excitation wavelength was 360 nm and the emission wavelength 440 nm. Unless otherwise indicated, the buffer was 50 mM Tris-HCl, pH 7.5 (25 °C), and the temperature of the cuvette was held at 25 °C with a water bath. To determine the affinity of the fluorophore (mAP5Am) and ATP to the enzyme, a solution of about 0.3 μM mAP5Am and different amounts of ATP (with 2.5 mM EDTA or 5 mM MgCl₂) in a final volume of about 1 mL (depending on the volume increments added to 1 mL of solution) was titrated with enzyme. The apparent affinities were fitted according to eq 1 (see below). A replot of these apparent affinities versus the ATP concentrations gives information on the dissociation constants (*K*) for both mAP5Am and ATP.

To determine the affinities of other ligands, a solution of enzyme and fluorophore was titrated with ligand, and the decrease of the fluorescence signal caused by the displacement of the fluorophore by the ligand was used together with the known *K* for mAP5Am and eq 2 or 3 (see below) to obtain the affinity for the ligand. In all cases the concentrations of the participating substances as well as the fluorescence intensity were corrected for the volume increments of every titration step. Fluorescence due to enzyme alone was less than 1% of the total signal and therefore negligible.

Equations for Fluorescence Titration Experiments. E_0 , M_0 , and L_0 are total concentrations of enzyme, fluorophore, and ligand, respectively, and E_f , M_f , and L_f are the corresponding free concentrations. EM and EL are the concentrations of the corresponding complexes. F_n is the fluorescence intensity of the *n*th titration step; F_0 and F_{max} represent the values for the signal of fluorophore alone and fluorophore saturated with protein.

Parameters were adjusted to the measured data with a nonlinear least-squares Simplex procedure. According to the magnitude of dissociation constants to be measured, one or more of the following procedures were used:

(I) *Addition of Enzyme to Fluorophore under Conditions Where E_0 , $M_0 \approx K_{\text{EM}}$ and One Binding Site Is Assumed.* With this method the affinity of the fluorophore to the enzyme will be determined directly. From the definition of the enzyme-fluorophore dissociation constant $K_{\text{EM}} = M_f E_f / \text{EM}$, it is easily shown that

$$\text{EM} = (E_0 + M_0 + K_{\text{EM}}) / 2 - \left([(E_0 + M_0 + K_{\text{EM}}) / 2]^2 + E_0 M_0 \right)^{1/2} \quad (1)$$

This equation will be abbreviated with $\text{EM}\{K_{\text{EM}}, M_0, E_0\}$ since

the actual concentration of the enzyme-fluorophore complex EM is a function of the three components in brackets. Therefore, the measured data points may be described by

$$F_n = (\text{EM}\{K_{\text{EM}}, M_0, E_0\} / M_0) (F_{\text{max}} - F_0) + F_0 \quad (2)$$

(II) *Addition of Competitive Substrate to Enzyme-Fluorophore Complex (Displacement).* It is assumed that the fluorophore has a high affinity for the enzyme, which means that M_0 does not equal M_f , but the substrate has to be in large excess over E_0 and M_0 , which means $L_0 \approx L_f$. For the following equation there are no special requirements concerning the conditions at the start of the experiment:

$$\text{EM}_0 = (E_0 + M_0 + K_{\text{EM}}) / 2 - \left([(E_0 + M_0 + K_{\text{EM}}) / 2]^2 + E_0 M_0 \right)^{1/2} \quad (3)$$

The equation gives the amount of enzyme-fluorophore complex as it would be without a competitive substrate present (i.e., the start of the experiment). For every titration step (*n*) the following holds:

$$\text{EM}_n = [E_0 + M_0 + K_{\text{EM}}(1 + L_0/K_{\text{EL}})] / 2 - \left([(E_0 + M_0 + K_{\text{EM}}(1 + L_0/K_{\text{EL}}))^2 + E_0 M_0] \right)^{1/2} \quad (4)$$

and thus

$$F_n = (\text{EM}_n / \text{EM}_0) (F_{\text{start}} - F_0) + F_0 \quad (5)$$

where F_{start} is the fluorescence of the enzyme-fluorophore mixture at the start of the experiment. K_{EM} must be known from other experiments in order to calculate the affinity for the competing ligand.

(III) *Addition of Competitive Substrate to the Enzyme-Fluorophore Complex with High Affinity of Fluorophore and Substrate to the Enzyme.* This means that in general neither the concentration of the free fluorophore nor that of the free ligand equals their respective total concentration. The affinity of the fluorophore to the enzyme has to be known as in (II). Evaluation of K_{EL} was by the following iterative procedure:

(Step A) *Initial Calculation of M_f and L_f at the Beginning of the Fitting Procedure.* From $M_f = M_0 - \text{EM}$ follows

$$M_f = M_0 - \text{EM}\{K_{\text{EM}}, M_0, E_0\} \quad (6)$$

and from $L_f = L_0 - \text{EL}$ follows

$$L_f = L_0 - \text{EL}\{K_{\text{EL}}, L_0, E_0\} \quad (7)$$

where K_{EL} must be a realistic estimate.

(Step B) *Fine Tuning of Free Concentrations.* The expressions for the dissociation constants are extended by the effect of the competitive counterpart:

$$M_f = M_0 - \text{EM}\{K_{\text{EM}}(1 + L_f/K_{\text{EL}}), M_0, E_0\} \quad (8)$$

$$L_f = L_0 - \text{EL}\{K_{\text{EL}}(1 + M_f/K_{\text{EM}}), L_0, E_0\} \quad (9)$$

This procedure is performed 10 times in a processing loop for every titration step and every new estimate of K_{EL} , F_0 , and F_{max} generated by the fitting procedure. Then, calculating the concentration of EM as it would be without inhibitor as in (II)

$$\text{EM}_0 = (E_0 + M_0 + K_{\text{EM}}) / 2 - \left([(E_0 + M_0 + K_{\text{EM}}) / 2]^2 + E_0 M_0 \right)^{1/2} \quad (10)$$

and finally calculating EM with inhibitor and the resulting fluorescence

$$\text{EM}_n = \text{EM}\{K_{\text{EM}}(1 + L_f/K_{\text{EL}}), M_0, E_0\} \quad (11)$$

$$F_n = (\text{EM}_n / \text{EM}_0) (F_{\text{start}} - F_0) + F_0 \quad (12)$$

Note that this procedure is valid for all concentrations of enzyme, ligands, and fluorophore.

Determination of Chemical Equilibrium. A solution of 300 μM AMP and 1000 μM ATP in a total volume of 1 mL of

50 mM Tris-HCl, pH 7.5, was incubated at 25 °C in the presence of 10 µg of adenylate kinase (≈0.5 µM enzyme) and 2 mM MgCl₂. Aliquots were analyzed on HPLC (see above) until no further change in the fractional amounts of substrates and products occurred. The resultant composition was 60.9% ATP, 28.9% ADP, and 9.6% AMP. This leads to an overall chemical equilibrium constant of $K^* [\text{ATP}][\text{AMP}]/[\text{ADP}]^2 = (790 \mu\text{M})(125 \mu\text{M})/(375 \mu\text{M})^2 = 0.7$.

Steady-State Kinetics. To measure the kinetic parameters in the forward reaction (production of ADP), a coupled colorimetric assay was used (Berghäuser, 1975), which was optimized for adenylate kinase of *E. coli* (Reinstein et al., 1988). The colorimetric assay in the backward direction (production of ATP and AMP) (Brune et al., 1985) was modified to vary the concentrations of ADP and Mg·ADP individually. The concentration of a MgCl₂ stock solution was assayed with a commercial test (Sigma) based on the use of calmagite (Chauhan & Sarkar, 1969). The dissociation constant of 250 µM for the interaction of Mg²⁺ with ADP (Morrison et al., 1961) was used to calculate the necessary amounts of total ADP and Mg to fix either ADP without Mg²⁺ or Mg·ADP while the other was varied. It should be noted that the Mg²⁺-complexing ability of NADPH present in the test was not taken into account. Also, the conditions used in the steady-state system are slightly different from those of Morrison. In both cases, 1 unit of enzymatic activity is defined as the consumption of 1 µmol of substrate by one binding site per minute.

Determination of Temperature Stability by Circular Dichroism. A fluorescence cuvette (0.4-cm path length) was filled with 1.5 mL of 10 mM phosphate buffer (pH 7.5) containing 0.3 mg of protein. Circular dichroism was recorded with a Jobin-Yvon Dichrograph Mark III at a fixed wavelength of 220 nm. The rate of temperature increase was 40 °C/h in a Haake F3 water bath. The temperature was measured directly in the cuvette. To determine the melting temperature, the following equation, which is based on the van't Hoff relation, was used [taken from Hecht et al. (1984)]:

$$\theta_T = \theta_D + (\theta_N - \theta_D)/(1 + f)$$

where $f = \exp[(\delta H_{\text{denat}}/RT)(T/T_m - 1)]$, θ_T is the ellipticity at temperature T (kelvin), θ_D is that of denatured protein and θ_N that of native protein, T_m is the melting temperature (kelvin), and δH_{denat} is the standard enthalpy of denaturation.

Determination of Temperature Stability by Fluorescence. Equal amounts of the fluorophore mAP5Am and purified enzyme were mixed at 25 °C in 1 mL of Tris-HCl buffer, pH 7.5 (25 °C), containing 2.5 mM EDTA and heated to 70 °C in about 40 min. The fluorescence signal was observed as described above. The decay of the fluorescence signal was analyzed with an equation describing the three main factors contributing to this decay.

(1) Heating a sample of free fluorophore results in a decay of signal that may be described by an exponential equation:

$$\delta F_n^{\text{quench}} = \delta F_{\text{quench}}^{\text{max}}(1 - \exp[-k_{\text{quench}}(T_n - T_0)])$$

where $\delta F_n^{\text{quench}}$ describes the difference between the signals F_0 (the fluorescence at the starting temperature T_0) and F_n (the fluorescence signal at any temperature point T_n), $\delta F_{\text{quench}}^{\text{max}}$ is the maximal quenching amplitude obtainable, and k_{quench} may be termed the temperature-quenching rate constant. The absolute value of $\delta F_{\text{quench}}^{\text{max}}$ is of course dependent on the initial fluorescence intensity, but in the concentration range of mAP5Am used, it was 0.75 times the initial fluorescence at 25 °C. It should be noted that enzyme-bound fluorophore is almost fully protected from quenching effects.

(2) The dissociation constant of enzyme-fluorophore complex is a function of temperature according to

$$K_{\text{EM}}(T_n) = K_{\text{EM}}(T_0) \exp[(\delta H_{\text{KEM}}/R)(1/T_n - 1/T_0)]$$

where δH_{KEM} is the standard enthalpy of the enzyme-mAP5Am equilibrium constant.

(3) The melting of the protein itself may be described by analogy to the equation used for CD measurements:

$$E_n(T_n) = E_0/\exp[(\delta H_{\text{denat}}/RT_n)(T_n/T_m - 1/T_0)] + 1$$

where $E_n(T_n)$ is the concentration of native enzyme as a function of temperature. Defining the relationship

$$\text{EM}\{K_{\text{EM}}, E, M\} = (K + E + M)/2 - \{[(K + E + M)/2]^2 - \text{EM}\}^{1/2}$$

which calculates the enzyme-mAP5Am complex concentrations for any given dissociation constant and the total enzyme and fluorophore concentrations and restricting the temperature quenching effect to free fluorophore

$$\delta F_{\text{quench}}(\text{cor}) = \delta F_{\text{quench}}(1 - \text{EM}/M_0)$$

the following equation relating the various parameters can be derived:

$$F_n(T_n) = F_0 + (F_{\text{max}} - F_0) \frac{\text{EM}\{K_{\text{EM}}(T_n), M_0, E_n(T_n)\}}{\text{EM}\{K_{\text{EM}}(T_0), M_0, E_0(T_0)\}} - \delta F_{\text{quench}}(\text{cor})$$

where F_0 is the fluorescence of free mAP5Am and F_{max} that of the fluorophore-enzyme complex at temperature T_0 (starting point). After calibration of the temperature quenching effects and measurement of the enzyme-fluorophore dissociation constant at 25 °C, only three unknown variables remain: δH_{denat} , δH_{KEM} , and T_m (the melting point). Although Tris is known to have a rather high temperature coefficient ($\delta\text{pH}/\text{deg C} = 0.025$), it was used since all kinetic data had been determined in this buffer.

Preparation of Sample for NMR. About 12–14 mg of protein was dialyzed twice against 20 mM potassium phosphate, pH 6.4, at 4 °C in the presence of the mixed-bed ion exchanger Amberlite ICR-718 (Serva). The resulting protein was freeze-dried, dissolved in 4 mL of D₂O (Merck) to exchange labile protons, and lyophilized again after 6 h of storage at 4 °C. The freeze-dried protein was redissolved in 0.5 mL of 99.9% D₂O (Sigma) before measurement, and the protein concentration was determined according to the method of Ehresmann et al. (1973). The nucleotide solution for titration experiments was also exchanged against D₂O and adjusted to pH 7.0 with NaOD.

NMR Measurements. Samples were measured in 5 mm diameter sample tubes on a Bruker AM500 spectrometer. The sample temperature was controlled at 300 K with a precooled stream of dry air that was temperature regulated with a standard Bruker VT1000 unit. The residual HDO resonance was suppressed by selective irradiation at the HDO frequency. Chemical shifts of protons are referenced to internal DSS (sodium 4,4-dimethyl-4-silapentane-1-sulfonate).

2D NMR Experiments. Two-dimension (2D) experiments were performed according to well-established procedures (Wüthrich, 1986). All 2D spectra were obtained in the phase-sensitive mode with quadrature detection in both dimensions with the time proportional phase incrementation technique (TPPI; Marion & Wüthrich, 1986). The residual water resonance was suppressed by permanent irradiation (except for the acquisition period) at the HDO frequency. Essential experimental parameters for NOESY experiments were 4K × 512 W frequency domain matrix, spectral width

Table I: Kinetic Constants of Mutant (Q28H) and Wild-Type AKec^a

	enzyme	K_m (μM)	V_{max} (units/mg)	k_{cat} (s^{-1})	k_{cat}/K_m ($\text{s}^{-1}\mu\text{M}^{-1}$)
Mg·ATP	WT	71	780	305	4.3
	Q28H	11	150	58.5	5.3
AMP	WT	26	770	300	11.6
	Q28H	7.5	240	93.6	12.5
Mg·ADP	WT	75	330	130	1.7
	Q28H	89	85	33	0.36
ADP	WT	4.0 (2.7) ^b	257	100	25
	Q28H	0.13 ^b	85 ^b	33 ^b	253 ^b

^aThe constants were measured under steady-state conditions with a coupled colorimetric test (see Materials and Methods). Concentrations for fixed substrates were as follows: AMP_{fix}, 300 μM for WT and 50 μM for Q28H; ATP_{fix}, 800 μM for wild-type AKec and 800 μM for Q28H; ADP_{fix}, 300 μM for wild-type AKec and 300 μM for Q28H; Mg·ADP_{fix}, 1 mM for wild-type AKec. One unit of enzymatic activity is defined as the consumption of 1 μmol of AMP or ADP per minute. ^bCalculated according to the Haldane (1930) equation, with $K^* = (k_{\text{cat}}/K_m)_{\text{ATP}}(k_{\text{cat}}/K_m)_{\text{AMP}}/(k_{\text{cat}}/K_m)_{\text{ADP}}^2$ and $K^* = [\text{ATP}][\text{AMP}]/[\text{ADP}]^2 = 0.7$.

500 MHz in either dimension, relaxation delay 1.2 s, $p/32$ -shifted sine-bell filter in the ω_1 dimension and $p/64$ -shifted sine-bell filter in the ω_2 dimension, and zero-filling to 1K in the ω_2 dimension before Fourier transformation.

RESULTS AND DISCUSSION

Mutagenesis and Protein Preparation. The mutation of Gln-28 to His by site-directed mutagenesis, using the "gapped-duplex" method of Kramer et al. (1984), resulted in 25% mutation efficiency. Wild-type protein and mutant protein Q28H were expressed in high amounts by use of a multicopy pEMBL plasmid harboring the AKec gene with its own promoter such that between 30 and 40% of the soluble extract consisted of adenylate kinase. Both proteins could be prepared to high purity with the methods described earlier (Reinstein et al., 1988).

Kinetic Properties. The steady-state parameters of both wild-type and mutant proteins were measured and are listed in Table I. The K_m values for ATP and AMP of the Q28H mutant are 11 and 7.5 μM and thus 6.5 and 3.5 times lower than those for wild-type protein.

K_m values for ADP of the *E. coli* adenylate kinase have been obtained previously by treating the kinetic data under the assumption that the two binding sites of ADP on the enzyme are identical (Su & Russell, 1968; Ito et al., 1980; Saint Girons et al., 1987; Reinstein et al., 1989). This treatment may produce misleading results since AK has two binding sites for adenine nucleotides with different affinities and specificities and also different specificities for the same ligand, depending on whether or not it is complexed to Mg^{2+} . Thus, in order to get an estimate of the K_m values for ADP and Mg·ADP individually, the known dissociation constant for the ADP·Mg complex (250 μM ; Morrison et al., 1961) was used to calculate the necessary total concentrations of ADP and MgCl_2 to fix either free ADP or ADP·Mg while increasing the concentration of the other. The K_m values for Mg·ADP are very similar for the wild-type and mutant proteins. The K_m values for metal-free ADP were difficult to measure for wild-type enzyme and impossible for Q28H with the coupled assay. The reason for this is a lag phase of about 20–30 s which is inherent to the coupled spectroscopic assay using HK and G6PDH (Roberts, 1977), so that an appreciable amount of ADP is depleted before a steady-state reaction is reached.

In order to calculate these values, the Haldane (1930) relationship was used, which correlates the four K_m values

(AMP, ATP·Mg, ADP, and ADP·Mg) and the two k_{cat} values for the forward and backward reaction and the overall chemical equilibrium constant (K^*) to obtain K_m for ADP:

$$K_m(\text{ADP}) = \frac{[k^*(\text{ADP}\cdot\text{Mg})k_{\text{cat}}(\text{ADP})/k^*(\text{AMP})k^*(\text{ATP}\cdot\text{Mg})]K^*}{[k^*(\text{ADP}\cdot\text{Mg})k_{\text{cat}}(\text{ADP})/k^*(\text{AMP})k^*(\text{ATP}\cdot\text{Mg})]K^*}$$

where $k^* = k_{\text{cat}}(\text{N})/K_m(\text{N})$ (N = nucleotide). The value for the equilibrium constant K^* was determined as described under Materials and Methods. It is 0.7 in the direction of ADP production and agrees well with the value of Markland and Wadkins (1966), who used catalytic amounts of AK from bovine liver mitochondria to measure the chemical equilibrium constants for different buffer conditions. The measured K_m values for Mg·ADP are similar to those for wild-type AKec and Q28H (75 and 89 μM , respectively) and are close to that of Mg·ATP for the wild-type enzyme. The K_m values for metal ion free ADP are shown in Table I. Again, the value for Q28H is much lower than for wild-type enzyme. Despite the fact that some simplifications were made in calculating the K_m values for ADP (see Materials and Methods), the measured and calculated $K_m(\text{ADP})$ for wild-type protein are very close.

AMP Is a Competitive Inhibitor for ATP. An additional difficulty associated with the determination of K_m values of adenylate kinase arises because AMP is a competitive inhibitor for the ATP binding site but not vice versa (Reinstein et al., 1988; Rhoads & Lowenstein, 1968). In order to get an estimate of the affinity of AMP for the ATP binding site, we performed experiments with [ATP] fixed at 800 μM and AMP increased to 100-fold over its K_m value. The data were fitted according to the following equation, which is valid for enzymes with a rapid equilibrium mechanism (Segel, 1975):

$$v = V_{\text{max}}[\text{AMP}]/K_m(\text{AMP}) \left(1 + \frac{K_m(\text{Mg}\cdot\text{ATP})}{[\text{Mg}\cdot\text{ATP}]} \right) + \frac{[\text{AMP}] \left[1 + \frac{K_m(\text{Mg}\cdot\text{ATP})}{[\text{Mg}\cdot\text{ATP}]} + \frac{K_m(\text{Mg}\cdot\text{ATP})(K_m(\text{AMP}) + [\text{AMP}])}{K_i(\text{AMP})[\text{Mg}\cdot\text{ATP}]} \right]}{K_i(\text{AMP})[\text{Mg}\cdot\text{ATP}]}$$

This equation is a simplified version of the original one since all binding events were taken to be independent of each other. The resulting K_i values were 360 μM for wild-type AKec and 120 μM for Q28H, which means that AMP has a kinetically significant affinity to the ATP binding site. It was also possible to show that Mg^{2+} -free ATP is a competitive inhibitor of Mg·ATP with a K_i of 32 μM for wild-type AKec and 8 μM for Q28H, taking K_{mgATP} as 40 μM (O'Sullivan & Perrin, 1961) and K_m values for Mg·ATP as listed in Table I.

Properties of Fluorescent Analogues of AP5A. Since there are no tryptophan residues in adenylate kinase of *E. coli* and therefore no strong intrinsic fluorescence signal which may be used to report ligand binding (as in AKy; Tomasselli & Noda, 1983), it was necessary to use a fluorescently labeled ligand for the spectroscopic measurement of ligand-protein interaction. *N*⁶-Etheno-AP5A produces no significant fluorescence enhancement on binding to *E. coli* adenylate kinase in contrast to mammalian cytosolic adenylate kinases (Feldhaus et al., 1975). Hiratsuka (1983) reported that adenosine triphosphates with an *N*-methylanthraniloyl (mant) group bound to the 2'- or 3'-hydroxyl of the ribose moiety via an ether linkage are substrates for AK1 from rabbit. In order to obtain a nonreactive fluorescent analogue for stable titration experiments, we synthesized derivatives of AP5A with one (mAP5A) or two (mAP5Am) riboses modified by *N*-methylanthraniloyl groups. The structural formula of

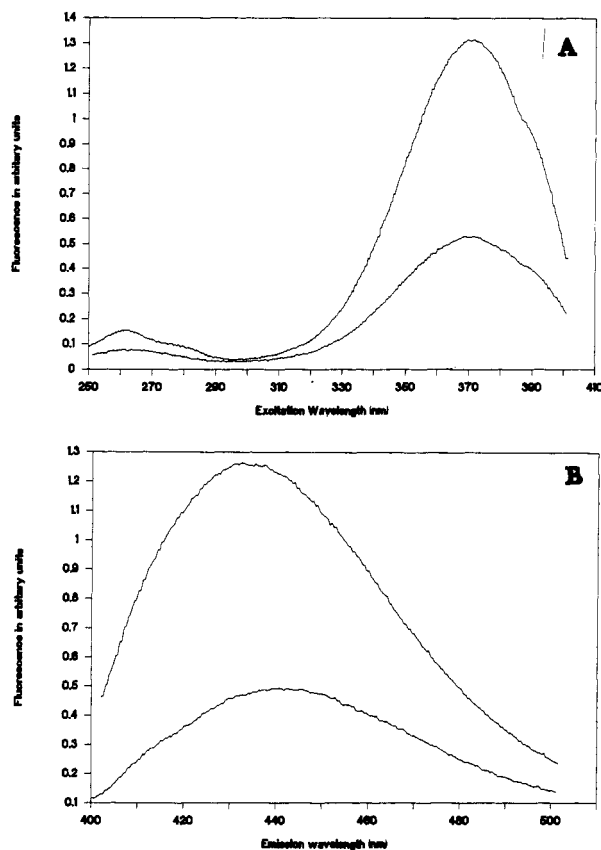


FIGURE 2: Excitation and emission spectra of mAP5Am at 25 °C, free (lower curve) and with wild-type enzyme (upper curve). The conditions of the experiment were 50 mM Tris-HCl, pH 7.5, 5 mM MgCl₂, 0.48 μM mAP5Am, and 1.8 μM wild-type enzyme. Concentration of the enzyme-fluorophore complex may be calculated to be 0.4 μM (fluorophore is saturated to 82%). Emission was recorded at a fixed excitation wavelength of 360 nm; fixed emission wavelength was 440 nm for the excitation spectra.

mAP5Am is shown in Figure 1.

This compound produces an exceptionally high fluorescence enhancement on binding to AKec (ca. 300%) and a blue shift of the emission wavelength of about 10 nm. Excitation and emission spectra of free mAP5Am and the wild-type AKec-mAP5Am complex are shown in Figure 2. It is noteworthy that the wavelength of the excitation maximum is far from the wavelength range where nucleotides absorb, so no quenching effects due to substrates occur. The maximal amplitudes obtained by the binding of mAP5A or mdATP with only one fluorescent group are 130% and 150%, respectively. It is also noteworthy that mdATP is a rather poor substrate for AKec with about 5% maximal catalytic rate compared to ATP. This is in contrast to the values reported for mATP and AK1 (rabbit) by Hiratsuka (1983). Holmes and Singer (1973), however, reported dATP to be equivalent to ATP with respect to its K_m and V_{max} values for AKec.

Active Site Titration with Fluorescent Analogue. In order to determine the number of binding sites for the fluorophore, active site titrations were performed. The addition of mAP5Am to wild-type AKec is shown in Figure 3. Two phases of increasing fluorescence can be clearly separated since the concentration of enzyme is well above the dissociation constant. Comparing the second phase with a titration of fluorophore alone indicates that this fluorescence increase is due to addition of free fluorophore alone. Adding enzyme to fluorophore under similar conditions also results in a biphasic curve, where the slope of the second phase is nearly zero. Comparing the protein concentration derived from this titration

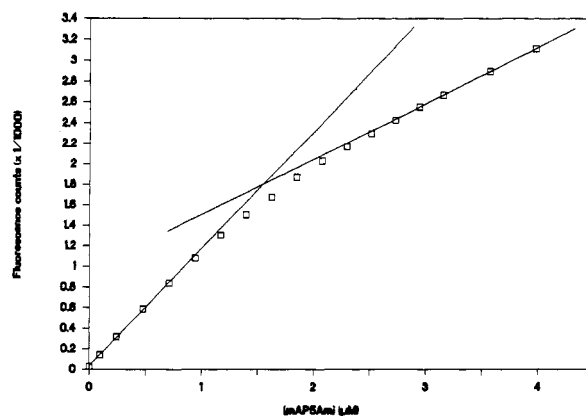


FIGURE 3: Active site titration of wild-type enzyme. Buffer used was 50 mM Tris-HCl containing 2.5 mM EDTA, 25 °C; concentration of enzyme at start was 1.77 μM [measured according to Bradford (see Materials and Methods)]; initial volume was 1015 μL. Interpolation of the two phases gives an intersection at [mAPAm] = 1.55 μM. The volume-corrected concentration of enzyme at this point is 1.71 μM. This indicates that 92% of the enzyme is able to bind the inhibitor.

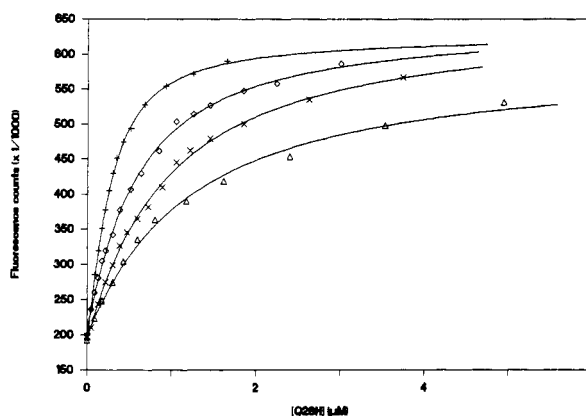


FIGURE 4: Addition of Q28H to a fixed amount of fluorophore mAP5Am with different initial concentrations of ATP. Conditions of the experiment were as follows: 50 mM Tris-HCl, 25 °C, 2.5 mM EDTA, initial volume 1 mL, 0.236 μM mAP5Am (in the case where [ATP] = 40 μM, it is lower for the higher ATP concentrations) and [ATP] = 40 μM (+), 155 μM (◇), 267 μM (×), and 377 μM (Δ). The observed dissociation constants for the enzyme-fluorophore complex (K_{EM}^{obs}) were fitted as described under Materials and Methods (eq 2). According to $K_{EM}^{obs} = K_{EM}(1 + [L]/K_{EL})$, which reflects competitive inhibition of fluorophore (M) by ligand (L), a replot of [L] versus K_{EM}^{obs} results in a straight line with K_{EM} as intercept and K_{EM}/K_{EL} as slope. The obtained dissociation constants are $K_{EM} = 0.045$ μM ($K_{Q28H-mAP5A}$) and $K_{EL} = 15.8$ μM ($K_{Q28H-ATP}$).

with that determined according to Bradford (1976) with BSA as standard shows that 92% enzyme is able to bind the analogue. Thus, we can conclude that within the limits of error the stoichiometry of binding is 1:1. This determination of the active site concentration avoids pitfalls in the analysis of binding of Scatchard plots or complicated mathematical treatments (Klotz, 1982; Bonnicie et al., 1988; Peters & Pin-goud, 1979).

Affinity between Fluorescent Ligand and Proteins. In order to determine whether the fluorescent analogues can be used to estimate the affinities of various substrates and whether this can be done in a suitable concentration range, we determined the affinity between enzyme (E) and mAP5Am (M). Figure 4 shows titrations where the mutant enzyme Q28H is added to 0.48 μM mAP5Am in the presence of different concentrations of ATP and 2.5 mM EDTA. One can see that this results in titration curves with slopes depending on the concentration of ATP, which is due to the competition between

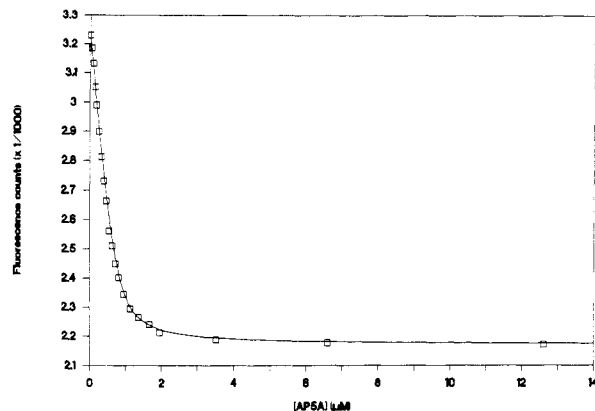


FIGURE 5: Displacement of mAP5Am from the mutant enzyme Q28H using AP5A. Conditions used in the experiment: 25 °C, 50 mM Tris-HCl buffer, pH 7.5, 5 mM MgCl₂, initial volume 1105 μL, initial [mAP5Am] 2.21 μM, initial [Q28H] 0.778 μM, and concentration of added AP5A solution 17.5 μM. Use of eq 3 (as described under Materials and Methods for strong ligand type) results in a K value of 0.88 nM for AP5A (using the known K of 0.03 μM for mAP5Am).

Table II: Dissociation Constants (μM) of Various Ligands and Fluorophores to Wild-Type and Mutant (Q28H) AKec^a

ligand	enzyme			
	WT		Q28H	
	5 mM MgCl ₂	2.5 mM EDTA	5 mM MgCl ₂	2.5 mM EDTA
mAP5Am	0.3	0.16	0.03	0.045
mAP5A	0.05			
mdATP	7.65	5.45		6.5
ATP	85	35	20	16
GTP	1510	407	600	
ADP		4.0		2.6
AMP		520		186
AP4A	43	13	0.7	1.3
AP5A	0.015	0.1	0.00088	0.0157
AP6A	0.108	0.16	0.008	0.03

^a The methods used to measure the affinities are given under Materials and Methods.

substrate and fluorescent analogue. Each curve is fitted according to eq 2 (see Materials and Methods) and yields an apparent dissociation constant. A replot of ligand concentrations versus observed dissociation constants for the enzyme-fluorophore complex (K_{app}^{EM}) results in a straight line, which indicates that ligand and fluorophore compete for the same binding site on the enzyme, and K_{EM} is determined by the intercept of this replot whereas K_{EM}/K_{EL} is determined by its slope.

Another indication that the fluorophore is a competitive inhibitor with regard to ATP originates from the fact that it is possible to reach maximal fluorescence under these conditions and/or that the ligand is able to displace the fluorophore from the enzyme. This is shown in Figure 5, where a complex between mutant enzyme and mAP5Am is titrated with increasing concentrations of unlabeled AP5A. One can see that the fluorescence decreases to the value expected for the free fluorophore. With the known binding constant of the fluorophore, one can calculate the affinity of the competitive ligand AP5A, which is 0.88 nM in the case of Q28H and 0.15 μM for the wild-type enzyme in the presence of MgCl₂ and 0.016 and 0.1 μM, respectively, in the presence of EDTA. Table II lists the results arising from the titration experiments. It is evident that the dissociation constants for Mg·ATP match the corresponding K_m values, and this is a strong indication of a rapid-equilibrium mechanism for AKec and, furthermore, supports the finding that the binding of substrates is inde-

Table III: Sum of Local Concentrations of AP5A ± MgCl₂ and AP6A ± MgCl₂ ($C_A + C_B$) Calculated from the Affinities for Substrates and Bisubstrate Inhibitors As Described under Results

	sum of local concn $C_A + C_B$ (M)			
	AP5A	Mg·AP5A	AP6A	Mg·AP6A
WT	0.009	0.12	0.0055	0.016
Q28H	0.009	0.09	0.005	0.01

pendent. The affinities for AMP are not identical with the corresponding K_m values. The reason for that will be discussed later.

Using the fluorophore, we find that the dissociation constants for GTP of about 1500 (wild-type AKec) and 600 μM (Q28H) in the presence of MgCl₂ are 20- or 30-fold weaker compared to those of ATP. With the coupled colorimetric steady-state test, the determination of the K_m value of a very weak binding ligand like GTP would be hampered by the production of ATP as the test proceeds. Thus, after some 30–60 s the reaction velocity is determined by the reaction of the natural substrate ATP, and it is impossible to get an accurate K_m value for the weak substrate.

The affinities for the multisubstrate inhibitors of APnA increase in the order AP4A < AP6A < AP5A. It is interesting to note that the affinity of AP5A for AKec is about 15-fold higher in the presence of Mg²⁺ than in its absence. The same order of affinities was also found for cytosolic adenylate kinases from rabbit and pig (Lienhard & Secemski, 1973; Feldhaus et al., 1975). The finding of Kupriyanov et al. (1986) that AK1 from rabbit is also able to catalyze the phosphate transfer from ADP to ATP to generate AP4 and AMP and the surprisingly high affinity for AP6A indicate that AK is able to tolerate ligands whose phosphate chain seems to be too long compared to the natural substrates. The dissociation constant of 0.015 μM for the binding of Mg·AP5A to the wild-type enzyme is 40-fold lower than the K_i value found by Saint Girons et al. (1987). The ratio of dissociation constants $K_{E-MgAP4A}/K_{E-MgAP5A}$ is 2850 for AKec. This corresponds to a concentration ratio of 3300 for 50% inhibition of AK1 rabbit with the same inhibitors (Lienhard & Secemski, 1973).

Analysis of Bisubstrate Inhibitor Binding. Since the rational design of enzymatic inhibitors is becoming more and more important (Broom, 1989) and multisubstrate inhibitors are especially promising in this respect, including AP5A and derivatives for AK isoenzymes or TP5A [α -(thymidine-5') ω -(adenosine-5') pentaphosphate] for thymidylate kinase (Hampton et al., 1982a,b), it is of interest to consider the effects that may contribute to the affinity of such inhibitors. An approach to an analogous problem was outlined for the binding of two-headed myosin to actin filaments by Goody and Holmes [1983; see also Jencks (1981)]. If one assumes that the binding of one functional part of the bisubstrate inhibitor increases the local concentration of the other, imaginary unbound counterpart and vice versa and defines these local concentrations as C_A and C_B using binding constants K_A and K_B for the substrates and K_{BI} for the inhibitor, the following equation can be derived:

$$K_{BI} = K_A + K_B + K_A(K_B C_B) + K_B(K_A C_A) \\ = K_A + K_B + K_A K_B (C_A + C_B)$$

It is possible for the local concentrations for the two functional parts to be different. To simplify this situation, we use $(C_A + C_B)/2$ as the mean concentration of the second half of the bisubstrate analogue. Applying this equation to the affinities of AP5A and AP6A to AKec and Q28H results in calculated local concentrations that are nearly identical for the two enzymes, although their affinities for substrates and inhibitors

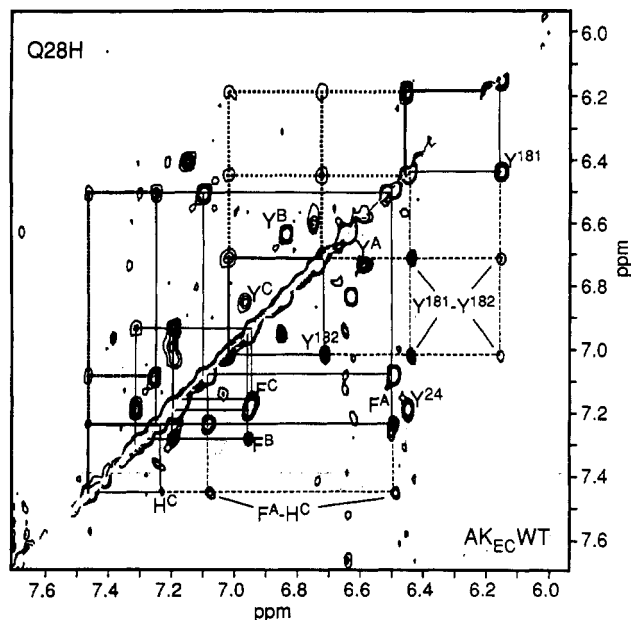


FIGURE 6: Aromatic ring proton resonance region of the 2D NOESY spectra of wild-type protein (below diagonal) and Q28H (above diagonal). Resonances were assigned according to Bock et al. (1988). Experimental conditions were 1.5 mM [WT], 1.5 mM [Q28H], 50 mM *N*-(2-hydroxyethyl)piperazine-*N'*-2-ethanesulfonic acid (HEPES), pH 8.0, and $T = 303$ K.

Table IV: Calculated Radii Using the Local Concentration of $(C_A + C_B)/8$ (Quarter Sphere) of AP5A \pm MgCl₂ and AP6A \pm MgCl₂ As Described under Results

	radii (Å)			
	AP5A	Mg-AP5A	AP6A	Mg-AP6A
WT	71	30	82	58
Q28H	69	32	86	76

are different (Table III). This result indicates that the binding modes of wild-type AKec and Q28H are very similar, a feature that is also apparent from one- and two-dimensional NMR experiments. The latter experiments also indicate that the overall structures of the two proteins are practically identical, as judged from 2D NOESY analysis of the aromatic residues (see Figure 6).

In order to correlate the effective local concentrations derived from the data with a mechanical model, we made the following considerations. If one functional part of the bisubstrate inhibitor is bound, its remaining imaginary free counterpart is freely movable in a restricted spatial area which may be described in a crude approximation as a quarter sphere. If we regard $(C_A + C_B)/8$ as the concentration which results from this quarter-sphere volume, then the corresponding radius should match (approximately, after all the simplifications) the half-length of the inhibitor (Table IV). From the summation of bond lengths the half-length of AP5A should be about 16–18 Å, whereas the calculated half-length from binding measurements is about 30 Å with Mg²⁺ and 70 Å without Mg²⁺, the discrepancy for AP6A being even greater. This calculation is obviously only a rather rough approximation. We interpret this result as a consequence of energetically unfavorable interactions (steric, electrostatic, or other) of the additional phosphate(s) in AP5A (AP6A).

This interpretation is supported by NMR data, which show that both adenines of APkA seem to be positioned properly (Vetter et al., 1990), and by studies on AKec mutant enzymes for which Mg-APa5A appears to be a virtually perfect inhibitor with respect to the considerations outlined above (Reinstein et al., 1990).

This approach may break down when the binding mode of substrates is strongly synergistic, but affinities of binary instead of ternary complexes are used. Nageswara Rao and Cohn (1977) noted a pronounced asymmetric binding of Mg-APkA to porcine AK in contrast to metal-free AP5A by using ³¹P NMR. This finding may indicate that the binding of Mg-AP5A is site directed as it is for metal-chelated and nonchelated substrates. The approach presented here allows calculation of the approximate predicted maximum binding strength for a bisubstrate inhibitor, on the basis of geometry, and can therefore be used as an indicator of the degree of "idealness" of an inhibitor.

Temperature Stabilities. In order to obtain information on the thermal stabilities of the two proteins investigated, we measured the denaturation behavior in two different types of experiments. These denaturation processes were almost completely reversible. CD measurements gave t_m values of 53.8 °C for wild-type AKec and 52.5 °C for Q28H and standard enthalpies of denaturation (δH_{denat}) of 472 kJ/mol for wild-type AKec and 460 kJ/mol for Q28H. The CD melting curves are shown in Figure 7A. The temperature stability for Q28H is thus very similar to that of the wild-type enzyme.

The fluorophore shown in Figure 1 can also be used to measure protein denaturation processes. We have devised a method to measure temperature stability of adenylate kinases in which the protein-fluorophore complex is heated and the decrease in fluorescence can be used to determine melting temperatures. Using this method (for details see Materials and Methods) results in values for the denaturation temperatures of 55.5 °C for wild-type AKec and 59.5 °C for Q28H and in values for the denaturation enthalpies (δH_{denat}) of 426 and 453 kJ/mol, respectively. The fluorescence melting curves are shown in Figure 7B. A melting temperature of 54 °C for wild-type AKec was found by Monnot et al. (1987). The discrepancy of the melting temperatures measured by this method and the CD method, which is small for wild type and most mutants analyzed [see Haase et al. (1989) and Reinstein et al. (1990)] and is somewhat larger for Q28H, is most probably due to the stabilizing effect of the fluorophore on the enzyme. We have measured the melting temperatures for different concentrations of mAPkAm and found a maximum stabilization of 9 °C due to the mAP5Am interaction (measured with $[mAP5Am] \gg K_{EM}$ at 25 °C; not applicable here, since $[mAP5Am] = ca. K_{EM}$). A similar value has been reported by Edge and Allewell (1988) with a stabilization of up to 7 °C for aspartate transcarbamoylase of *E. coli* and the ligand *N*-(phosphonoacetyl)-*L*-aspartate (PALA).

In spite of the discrepancies, there are some advantages of the fluorescence method. The melting process of the protein is now clearly defined as the loss of the capacity to bind ligand, which means that the denaturation of the active center is explicitly recorded and the definition of the melting process is functional rather than phenomenologic. Also, the renaturation of protein on cooling can be visualized as the ability to rebind the fluorophore and is thus an indication of the integrity of the active site after refolding. The high specificity and binding capacity of mAP5Am make it possible to measure the denaturation of adenylate kinase even in crude cell lysates of *E. coli* cells. This is shown in Figure 7C for a crude extract from a strain overproducing wild-type adenylate kinase (SMH50/-pEAK90). Analysis of this experiment leads to $t_m = 55.6$ °C and $\delta H_{denat} = 430$ kJ/mol, which are close to the values for the purified protein (55.5 °C and 425 kJ/mol, respectively). We thus regard this method as a practical and valuable tool that has its own merits and can, in combination

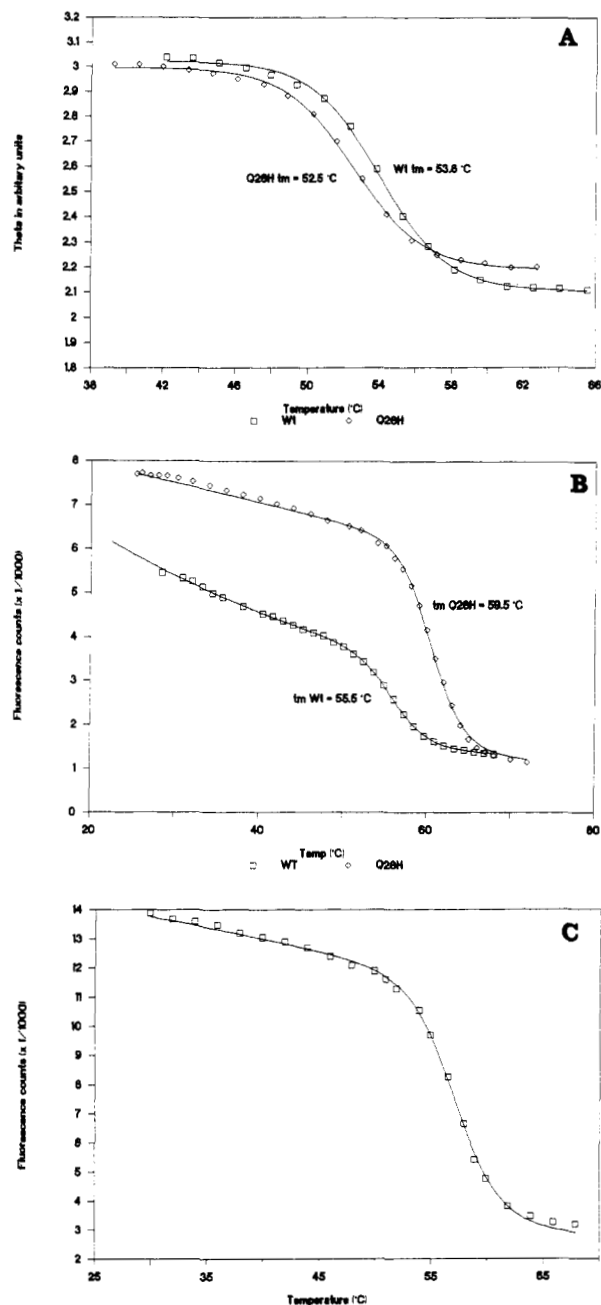


FIGURE 7: (A) CD melting curves of wild-type AKec and Q28H. Change of ellipticity was recorded as a function of temperature. Protein concentrations are 0.1 mg/mL in 10 mM KP_i buffer, pH 7.45. (B) Fluorescence melting curves of wild-type AKec and Q28H. Fluorescence intensity was recorded as a function of temperature, and buffer used in the experiment was 50 mM Tris-HCl, pH 7.5 at 25 °C, containing 2.5 mM EDTA; protein concentrations were 0.64 μM wild-type AKec and 0.42 μM Q28H; concentrations of fluorophores for wild-type AKec and mutant protein were 0.72 and 0.3 μM , respectively. The curves were adjusted to the same fluorescence counts for free fluorophore. (C) Fluorescence melting curve of crude *E. coli* extract containing wild-type protein. Total amount of protein in crude extract is 1 mg/mL. Taking the relative amount of AK as 20% of the total soluble protein (as judged by SDS gel electrophoresis), the concentration of adenylate kinase in crude extract may be calculated to be 0.2 mg/mL ($\approx 10 \mu\text{M}$). Conditions: 1 mL 50 mM of Tris-HCl, pH 7.5, + 160 μL of crude extract with $[\text{AK}] \approx 1.3 \mu\text{M}$ and $[\text{mAP5Am}] = 0.5 \mu\text{M}$.

with CD and scanning microcalorimetry (Privalov, 1980), give valuable information about stability and denaturation of proteins.

Analysis of AMP Binding by NMR. The most likely interpretation of kinetic and binding experiments is that AMP is able to bind to both sites of *E. coli* adenylate kinase with

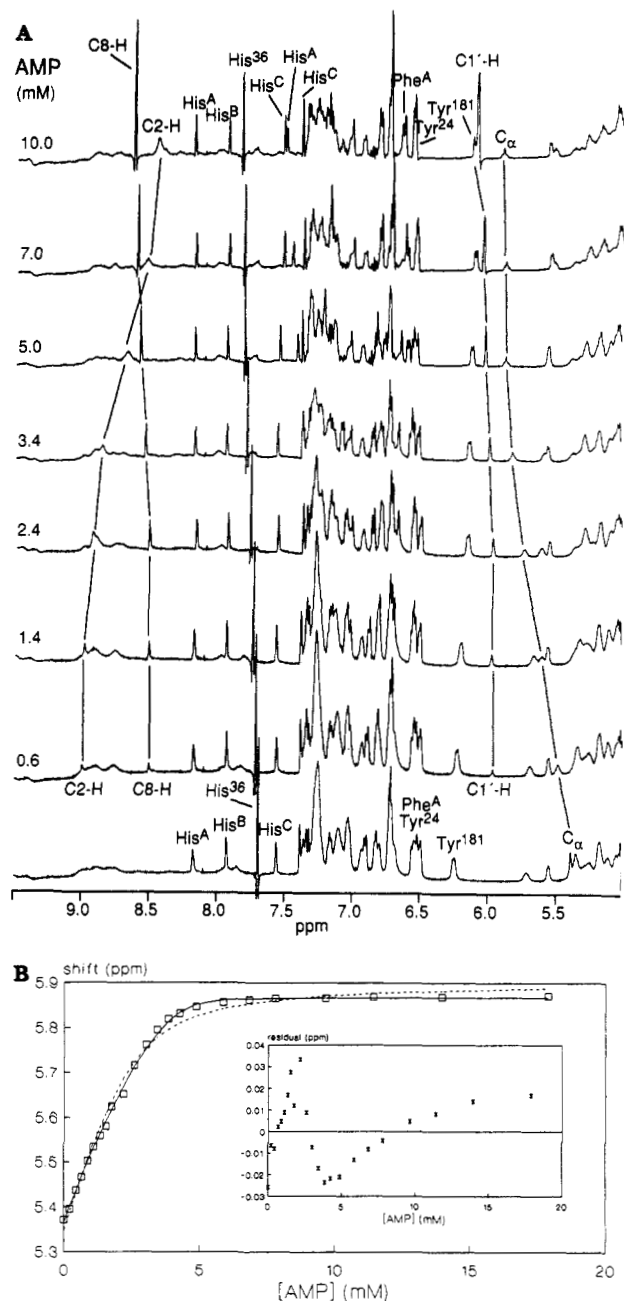


FIGURE 8: Titration of AMP with mutant enzyme Q28H. (A) Aromatic portion of the proton NMR spectrum of Q28H as a function of increasing AMP concentration (only 9 out of 23 titration steps are indicated). One well-resolved yet unassigned C α proton resonance shows one of the most pronounced shifts in the aromatic region. The initial concentration of Q28H was 2.4 mM; AMP concentration of each spectrum was as indicated. Enzyme and nucleotide solutions were prepared as described under Materials and Methods. (B) Chemical shift of a yet unassigned C α proton resonance as a function of the total AMP concentration. The data points were fitted according to a one-site binding model ($K = 480 \mu\text{M}$, dashed line) and to a two-site binding model (solid line, $K_1 = 24 \mu\text{M}$ and $K_2 = 73 \mu\text{M}$) where binding events are assumed to be independent. The residuals of the one-site fit are shown in the inset. It is evident that large systematic deviations occur.

high affinity. It was thus of interest to observe the effect of adding AMP to AKec on defined proton resonances of the enzyme. Figure 8A shows the "aromatic region" of Q28H in a titration experiment with AMP. All resonances in the aromatic part are in fast exchange between the free and bound forms. The resonances with the most pronounced chemical shifts that are separated well enough to be followed during the titration experiment are those of Tyr-181 (C3/5-H), which

was assigned by Bock et al. (1988), at 6.22 ppm and that of the newly introduced His-28 (C2-H) and an unassigned α proton at 7.84 and 5.37 ppm, respectively. As a representative example, the dependence of the chemical shift value of the α proton as a function of total AMP concentration is shown in Figure 8B. Assuming a model with only one binding constant, these data give a poor fit with obvious systematic deviations (Figure 8B). This quality of the fit was greatly enhanced when a mathematical expression for two nonequivalent binding sites was used. However, the accuracy of the evaluated K values in this titration experiment, with an initial concentration of one compound (the enzyme in this case) of about 20 times over the expected K (K_i^{AMP}), is bound to yield a rather crude approximation for the dissociation constant. This NMR experiment is therefore not suitable for determination of K values but nevertheless indicates that there are at least two different binding sites for AMP. The chemical shifts of the selected amino acid (and those of other amino acids which are not shown here) are induced by conformational changes of the protein due to binding of AMP to both sites. The movement of resonances due to addition of AMP observed here is very similar to those of the wild-type enzyme (Bock et al., 1988; Vetter et al., 1990).

CONCLUSIONS

Ligand binding analysis with AKec enzymes using fluorescence methods in combination with steady-state kinetics and NMR investigations leads to the following conclusions:

(1) The substrate AMP binds to both nucleotide binding sites of AKec inducing conformational changes in both binding events.

(2) ATP binds to the ATP site even without Mg^{2+} . The affinity is higher than in the presence of Mg^{2+} .

(3) AP5A seems to bind to both nucleotide binding sites on the enzyme although it is not a perfect bisubstrate inhibitor for AKec and Q28H as judged by its binding behavior compared to those of the substrates.

(4) The fluorophore mAP5Am does not bind to the AMP site in a proper way since it is not possible to displace mAP5Am by binding of AMP to its specific site alone. This may be due to the high specificity of the AMP site. Comparing the affinities for mdATP with those of mAP5A indicates that the presence of the fluorescently labeled ribose prevents the compound mAP5A from binding in a proper bisubstrate inhibitor mode. This interpretation is supported by the fact that mdATP is a rather poor substrate and therefore also seems to be positioned incorrectly. dATP is just as good a substrate as ATP for AKec (Holmes & Singer, 1972).

The mutant protein Q28H has the same temperature stability as wild-type AKec with an unaltered global structure compared to wild type as judged by NMR. Kinetic and binding effects on replacing glutamine 28 in AKec by histidine are opposite to those seen on replacing His-36 by Gln-36 in cytosolic adenylate kinase from chicken (Tian et al., 1988) but almost the same in magnitude, suggesting that there is a conserved structural environment which propagates these effects. The interaction of His-36 with Asp-93 (a highly conserved amino acid in all adenylate kinases) in AK1 (Asp-84 in AKec) has been discussed as contributing to the induced-fit mechanism of adenylate kinase by Dreusicke and Schulz (1988) and Tian et al. (1988). The distance of Gln-28 (NE2) to Asp84 (OD1) in AKec (4.1 Å) and that of N3 of His-36 to O1 of Asp-93 in AK1 pig (3.0 Å) are comparable, and it may be supposed that this interaction (called the conserved environment above) is responsible for the similarity of effects

on replacing His-36 by Gln and Gln-28 by His.

The interpretation that these amino acid exchanges produce slight perturbations in the interactions which are responsible for the induced-fit mechanism of adenylate kinases is further supported by the fact that these conversions alter K_m values for MgATP and AMP by about the same factor as wild-type AKec (Reinstein et al., 1988). Considering the rather minor effects of replacing His-36 by Gly in AK1 chicken (Tian et al., 1988) suggests that this interaction is not essential.

ACKNOWLEDGMENTS

We thank Marija Isakov for excellent technical assistance, G. E. Schulz for generously providing us with the coordinates of the structure of the AKec-AP5A complex, and K. C. Holmes for support.

Registry No. AK, 9013-02-9; MgATP, 1476-84-2; AMP, 61-19-8; MgADP, 7384-99-8; ADP, 58-64-0; ATP, 56-65-5; GTP, 86-01-1; mAP5Am, 128053-72-5; mAP5A, 128113-57-5; mdATP, 128113-53-1; AP4A, 5542-28-9; AP5A, 41708-91-2; AP6A, 56983-23-4; methylisatoic acid anhydride, 10328-92-4; glutamine, 56-85-9.

REFERENCES

- Berghäuser, J. (1975) *Biochim. Biophys. Acta* 397, 370-376.
 Bock, I., Reinstein, J., Brune, M., Wittinghofer, A., & Rösch, P. (1988) *J. Mol. Biol.* 200, 745-748.
 Bonniec, B., Sauloy, J., Ducrocq, R., & Elion, J. (1988) *Anal. Biochem.* 174, 280-290.
 Bradford, M. (1976) *Anal. Biochem.* 72, 248-254.
 Broom, A. D. (1989) *J. Med. Chem.* 32, 2-7.
 Brune, M., Schuhmann, R., & Wittinghofer, F. (1985) *Nucleic Acids Res.* 13, 7139-7151.
 Chauhan, U. P. S., & Sarkar, B. C. R. (1969) *Anal. Biochem.* 32, 70-80.
 Dente, L., Cesarini, G., & Cortese, R. (1983) *Nucleic Acids Res.* 11, 1645-1655.
 Dreusicke, D., & Schulz, G. E. (1988) *J. Mol. Biol.* 203, 1021-1028.
 Edge, V., & Allewell, N. M. (1988) *Biochemistry* 27, 8081-8087.
 Egner, U., Tomasselli, A. G., & Schulz, G. E. (1987) *J. Mol. Biol.* 195, 649-658.
 Ehresmann, B., Imbault, P., & Weil, J. H. (1973) *Anal. Biochem.* 54, 454-463.
 Feldhaus, P., Fröhlich, T., Goody, R. S., Isakov, M., & Schirmer, R. H. (1975) *Eur. J. Biochem.* 57, 197-204.
 Goody, R. S., & Holmes, K. C. (1983) *Biochim. Biophys. Acta* 726, 13-39.
 Haase, G. H. W., Brune, M., Reinstein, J., Pai, E. F., Pingoud, A., & Wittinghofer, A. (1989) *J. Mol. Biol.* 207, 151-162.
 Haldane, J. B. S. (1930) *Enzymes*, Longmanns, Green and Co., New York, (reprinted 1965, MIT Press, Cambridge, MA).
 Hampton, A., Chawla, R. R., & Kappler, F. (1982a) *J. Med. Chem.* 25, 644-649.
 Hampton, A., Kappler, F., & Picker, D. (1982b) *J. Med. Chem.* 25, 638-644.
 Hanes, C. S. (1923) *Biochem. J.* 26, 1406.
 Hecht, M. H., Sturtevant, J. S., & Sauer, R. T. (1984) *Proc. Natl. Acad. Sci. U.S.A.* 81, 5685-5689.
 Hiratsuka, T. (1983) *Biochim. Biophys. Acta* 724, 496-508.
 Hoard, D. E., & Ott, D. G. (1965) *J. Am. Chem. Soc.* 87, 1785-1788.
 Holmes, R. K., & Singer, M. F. (1973) *J. Biol. Chem.* 248, 2014-2012.
 Ito, Y., Tomasselli, A. G., & Noda, L. H. (1980) *Eur. J. Biochem.* 105, 85-92.

- Jencks, W. P. (1981) *Proc. Natl. Acad. Sci. U.S.A.* 78, 4046-4050.
- Klotz, I. M. (1982) *Science* 217, 1247-1249.
- Konrad, M. (1988) *J. Biol. Chem.* 263, 19468-19474.
- Kramer, M., Drutsa, V., Jansen, H. W., Kramer, B., Pflugfelder, M., & Fritz, H.-J. (1984) *Nucleic Acids Res.* 12, 9441-9456.
- Kupriyanov, V. V., Ferretti, J. A., & Balaban, R. S. (1986) *Biochim. Biophys. Acta* 869, 107-111.
- Lienhard, E. G., & Secemski, I. I. (1973) *J. Biol. Chem.* 248, 1121-1123.
- Mandel, M., & Higa, A. (1970) *J. Mol. Biol.* 53, 159-162.
- Maniatis, T., Fritsch, E. F., & Sambrook, J. (1982) *Molecular Cloning*, Cold Spring Harbor Laboratory, Cold Spring Harbor, NY.
- Marion, D., & Wüthrich, K. (1983) *Biochem. Biophys. Res. Commun.* 113, 967-974.
- Markland, F. S., & Wadkins, C. L. (1966) *J. Biol. Chem.* 241, 4136-4145.
- Maxam, A. M., & Gilbert, W. (1980) *Methods Enzymol.* 65, 499-560.
- McDonald, G. G., & Cohn, M. (1975) *J. Biol. Chem.* 250, 6947-6954.
- Mildvan, A. S. (1989) *FASEB J.* 3, 1705-1714.
- Monnot, M., Gilles, A.-M., Saint Girons, I., Michelson, S., Bârzu, O., & Femandjian, S. (1987) *J. Biol. Chem.* 262, 2502-2506.
- Morrison, J. F., O'Sullivan, W. J., & Ogston, A. G. (1961) *Biochim. Biophys. Acta* 52, 82-85.
- Müller, C., & Schulz, G. E. (1988) *J. Mol. Biol.* 202, 909-912.
- Nageswara Rao, B. N., & Cohn, M. (1977) *Proc. Natl. Acad. Sci. U.S.A.* 74, 5355-5357.
- Nageswara Rao, B. N., & Cohn, M. (1978) *J. Biol. Chem.* 253, 1149-1158.
- Noda, L. H. (1973) *Enzymes (3rd Ed.)* 8, 279-305.
- O'Sullivan, W. J., & Perrin, D. D. (1961) *Biochim. Biophys. Acta* 52, 612-614.
- Pai, E. F., Sachsenheimer, W., Schirmer, R. H., & Schulz, G. E. (1977) *J. Mol. Biol.* 114, 37-45.
- Peters, F., & Pingoud, A. (1979) *Int. J. Bio-Med. Comput.* 10, 401-415.
- Piantini, U., Sorensen, O. W., & Ernst, R. R. (1982) *J. Am. Chem. Soc.* 104, 6800-6801.
- Privalov, P. L. (1980) *Pure Appl. Chem.* 52, 479-497.
- Reinstein, J., Brune, M., & Wittinghofer, A. (1988) *Biochemistry* 27, 4712-4720.
- Reinstein, J., Gilles, A.-M., Rose, T., Wittinghofer, A., Saint Girons, I., Bârzu, O., Surewicz, W. K., & Mantsch, H. H. (1989) *J. Mol. Biol.* 264, 8107-8112.
- Reinstein, J., Schlichting, I., & Wittinghofer, A. (1990) *Biochemistry* (second paper of three in this issue).
- Rhoads, G., & Lowenstein, J. M. (1968) *J. Biol. Chem.* 243, 3963-3972.
- Richard, J. P., & Frey, P. A. (1978) *J. Am. Chem. Soc.* 100, 7757-7758.
- Roberts, D. V. (1977) *Enzyme Kinetics*. p 231, Cambridge University Press, Cambridge, U.K.
- Rösch, P., Klaus, W., Auer, M., & Goody, R. S. (1989) *Biochemistry* 28, 4318-4325.
- Rosenthal, A., Jung, R. R., & Hunger, H.-D. (1986) *Gene* 42, 1-9.
- Saint Girons, I., Gilles, A.-M., Margarita, D., Michelson, S., Monnot, M., Femandjian, S., Danchin, A., & Bârzu, O. (1987) *J. Biol. Chem.* 262, 622-629.
- Sanger, F., Nicklen, S., & Coulson, A. R. (1977) *Proc. Natl. Acad. Sci. U.S.A.* 74, 5463-5467.
- Schulz, G. E., Elzinga, M., Marx, F., & Schirmer, R. H. (1974) *Nature (London)* 250, 120-123.
- Schulz, G. E., Schiltz, E., Tomasselli, A. G., Frank, A. G., Brune, M., Wittinghofer, A., & Schirmer, R. H. (1986) *Eur. J. Biochem.* 161, 127-132.
- Segel, I. H. (1975) *Enzyme Kinetics*, p 314, Wiley, New York.
- Shaka, A. J., & Freeman, R. (1983) *J. Magn. Reson.* 51, 169-173.
- Spürgin, P., Tomasselli, A. G., & Schiltz, E. (1989) *Eur. J. Biochem.* 179, 621-628.
- Su, S., & Russell, P. J. (1968) *J. Biol. Chem.* 243, 3826-3833.
- Taylor, J. W., Ott, J., & Eckstein, F. (1985) *Nucleic Acids Res.* 13, 8765-8785.
- Thompson, H. T., Cass, K. H., & Stellwagen, E. (1975) *Proc. Natl. Acad. Sci. U.S.A.* 72, 669-672.
- Tian, G., Sanders, C. R., Kishi, F., Nakazawa, A., & Tsai, M.-D. (1988) *Biochemistry* 27, 5544-5552.
- Tomasselli, A. G., & Noda, L. H. (1983) *Eur. J. Biochem.* 132, 109-115.
- Vetter, I. R., Reinstein, J., & Rösch, P. (1990) *Biochemistry* (third paper of three in this issue).
- Wüthrich, K. (1986) *NMR of Proteins and Nucleic Acids*, Wiley, New York.
- Yanisch-Perron, C., Vieira, J., & Messing, J. (1985) *Gene* 33, 103-119.